Michelson Interferometry

Irtaza Tanveer Ahmad
Roll Number: 2024-10-0039
BS Physics
Syed Babar Ali School of Science and Engineering
Lahore University of Management Sciences

Abstract

This experiment introduces the foundations of optical interferometry using the Michelson Interferometer. Two primary experiments were conducted. The first experiment involved determining the wavelength of the light emitted from the laser. The second experiment involved determining the index of refraction of a glass slide of a specified thickness. A great deal of agreement was found between the experimental results and previously known results for both experiments.

1 Introduction to Interferometry

Broadly speaking, interferometry encompasses a number of techniques that utilise the phenomenon of superimposed waves interfering with one another to extract useful information. Interferometry experiments are commonplace in various fields of physics, including astronomy, fiber optic, plasma physics and nuclear physics to name a few. Interferometers exploit the wave phenomenon of interference, the addition of two waves to yield a resultant wave. This is a straightforward consequence of the linearity of the Wave Equation

$$\frac{\partial^2 f}{\partial x^2} = \frac{1}{v^2}\frac{\partial^2 f}{\partial t^2}. \tag{1}$$

Linearity in this context refers to the idea that a linear combination of two solutions $\psi(x,t)$ and $\chi(x,t)$ is also a solution. This is an immediate consequence of the fact that partial differentiation is linear.

The most common wave that is utilised in interferometry experiments is light; this is one of the reasons why the interferometer is also sometimes called the optical interferometer. The interference of light as a result of optical path differences and the resultant fringe patterns that arise is a well-studied phenomenon, and is the primary physical basis for a number of well-known interferometers, including the Michelson, Mach–Zehnder, and the Fabry–Perot interferometers.

In the study of optical interference, the central question is this: What are the conditions for interference between two beams of light which result in a stable pattern that can be appropriately analysed? One condition is the two beams must have nearly the same frequency. If this condition is not satisfied, then the phase difference between the two beams would vary with respect to time so rapidly that an interference pattern would not be observed. Another condition is that the two beams must be coherent i.e. the relationship between their phases must remain constant. Another consideration is whether the sources are monochromatic; strictly speaking however, this is not necessary but allows for much clearer interference patterns [3]. An example of polychromatic interference of light is seen in the rainbow colour pattern that is observed when oil is poured over water.

2 The Michelson Interferometer

The Michelson Interferometer was the first ever optical interferometer, invented in 1881 by Albert A. Michelson. It was later used in the famous Michelson-Morley Experiment which disproved the existence of an omnipresent ether through which light was thought to propagate through and validated Albert Einstein's Theory of Special Relativity [5]. The Michelson interferometer has many other diverse applications however. These include measuring the wavelength and spectral width of atomic emission lines, defining the meter in terms of the wavelength of light, measuring the diameters of stars, and measuring the thickness and surface features of microscopically thin films [6].

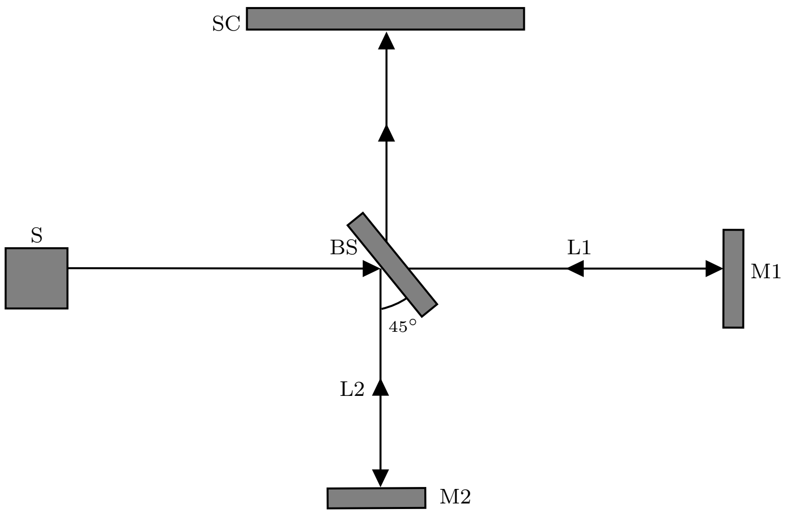

Figure 1: A simplified diagram of the Michelson Interferometer. S = light source, BS = beam splitter, M2 = fixed mirror, M1 = movable mirror, SC = viewing screen

The diagram above shows a schematic diagram of the Michelson Interferometer. The way it works is fairly simple. Light that is emitted from the source labelled S is passed through a beam splitter labelled BS. The beam splitter, as its name suggests, splits the beam into two parts. One beam passes through and propagates towards a mirror labelled M1 that can be movable by means of a computer controlled servo motor. This beam is reflected and the reflected beam, denoted by L1, propagates towards the beam splitter. The other beam is reflected by the beam splitter and propagates towards a second mirror labelled M2 that is fixed in position. The reflected beam labelled L2 travels towards the beam splitter, where it superimposes with the beam L1. The resultant output beam then propagates towards the screen. This output beam includes light rays that have optical path differences between them, which is why they demonstrate interference and a pattern will be observed on the screen. If a monochromatic light source is used and the mirrors are aligned correctly, a pattern of circular bright and dark fringes will be observed. The bright fringes correspond to constructive interference. The dark fringes correspond to destructive interference [1].

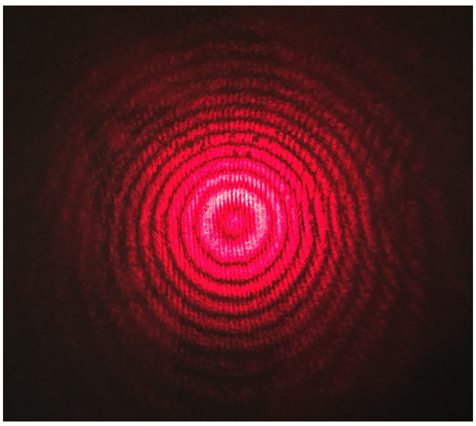

Figure 2: A picture of the interference patterns that were initially obtained

3 Determining the Wavelength of a Laser

3.1 Theoretical Background

The relative phase of the two beams L1 and L2 when they meet at the viewing screen depends on the difference in the length of their optical paths in reaching that point. It is a well-known result from optics that the condition for two beams to constructively interfere translates to

$$\Delta = m\lambda, \tag{2}$$

where Δ is the path length difference between the two beams, λ is the wavelength of the source and m is an integer. It is also known that the condition for destructive interference translates to the following equation [6]:

$$\Delta = \left(m + \frac{1}{2}\right)\lambda. \tag{3}$$

By moving M1, the path length of L1 can be varied. Since the beam traverses the path between M1 and the beam-splitter twice, moving M1 a quarter of the wavelength nearer the beam-splitter will reduce the optical path of that beam by half of the wavelength. As a result, destructive interference will be seen where originally constructive interference was seen, and dark fringes will be seen at positions where originally there were bright fringes. If M1 is moved an additional quarter of the wavelength closer to the beam-splitter, the new arrangement will be identical to the original. Hence, the mirror can be continuously moved in order to see the fringe pattern change from bright to dark, then back to bright and so on [1].

3.2 Experimental Procedure

3.2.1 Overview

The idea striaghtforward: first, a reference point is fixed on the screen. For convenience, this can be taken to be a point where there is a bright fringe. Once the reference point has been fixed, the mirror is moved some fixed distance Δd using a computer controlled servo motor and the number of fringes N that appear/disappear is counted. To be more specific, the number N corresponds to the number of times a bright fringe appears at the specified reference point. For one fringe to appear/disappear, the mirror must be moved through a distance of half a wavelength [1]. Knowing this, the following equation can be written

$$\Delta d = \frac{N\lambda}{2}. \tag{4}$$

Making N the subject, the following equation is obtained

$$N = \frac{2\Delta d}{\lambda}. \tag{5}$$

From Equation (5), it can be noted that there will be a linear relationship between N and Δd with a proportionality constant of $\frac{2}{\lambda}$. Hence, the idea is to take a fixed number of measurements of Δd and N, construct a Python plot with N on the y-axis and Δd on the x-axis (since N is the dependent variable and Δd is the independent variable in this context) using least-squares curve fitting and determine λ from the gradient m of the line

$$m = \frac{2}{\lambda}. \tag{6}$$

Making λ the subject of the formula above yields

$$\lambda = \frac{2}{m}. \tag{7}$$

3.2.2 Error Analysis

From Equation (7), the uncertainty in λ can be determined using the general error propagation formula

$$u_f^2 = \sum_i^n \left(\frac{\partial f}{\partial x_i}\right)^2 u_{x_i}^2, \tag{8}$$

where $f = f(x_1, x_2, \dots x_n)$, u_f is the uncertainty in f and u_{x_i} is the uncertainty in the variable x_i that f depends on [2]. Applying this formula to Equation (7) yields

$$u_\lambda^2 = \frac{4u_m^2}{m^4}. \tag{9}$$

In the above equation, u_λ denotes the uncertainty in λ and u_m denotes the uncertainty in the gradient of the least-squares fit line.
In order to determine u_m, the Polyfit function in Python's NumPy library can be utilised. This function can evaluate for the fit parameters for the data using the least-squares method and also construct the covariance matrix for the fit parameters. It is known that the error of the parameters is the square root of the diagonal entries of the covariance matrix [7]. Hence, it is a trivial matter to to determine u_m once the covariance matrix has been determined.

3.3 Experimental Results

5 measurements of Δd and N were taken. These measurements are shown in the table below, which also includes the uncertainty in each measurement of Δd due to the least count of the computer-controlled servo motor.

Δd (10^{-9}m)	N
5000 ± 9	16
10000 ± 9	31
15000 ± 9	44
20000 ± 9	63
25000 ± 9	78

Table 1: Measurements of Δd and N, including the uncertainty in each measurement of Δd

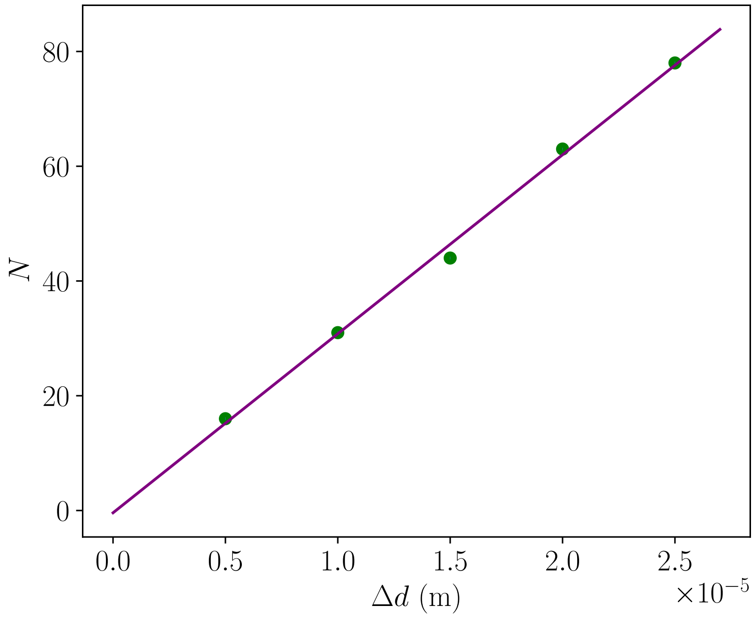

Figure 3: Plot of N versus Δd, including the line of best fit

The Python plot shown above displays the tabulated data points and the line of best fit that was obtained using the Polyfit function in NumPy. Using this function, the gradient of the line alongside its uncertainty, after rounding off to an appropriate number of significant figures, were determined to be

$$m = (3.12 \pm 0.10) \times 10^6 \text{m}^{-1}. \tag{10}$$

Using Equations (7) and (9), the wavelength and its associated uncertainty were determined to be

$$\lambda = (641 \pm 21)\text{nm}. \tag{11}$$

3.4 Discussion of Experimental Results

The laser that was used in the experiment was red in colour, and it is known that the wavelength of red light lies in the range of 630nm to 670nm. So, broadly speaking, the experimentally determined value of the wavelength does agree with the boundaries set by the actual known results from before. The experimental wavelength was also compared with the wavelength of the Thor Labs HeNe laser of 632.8nm. This resulted in a percentage discrepancy of 1.3%. Two major sources of uncertainty that were identified were:

1. The stability of the optical breadboard, which caused the apparatus to move about their fixed positions which could have affected the fringe patterns.

2. The human reaction time error in measuring the number of fringes.

4 Determining the Refractive Index of Glass

4.1 Theoretical Background

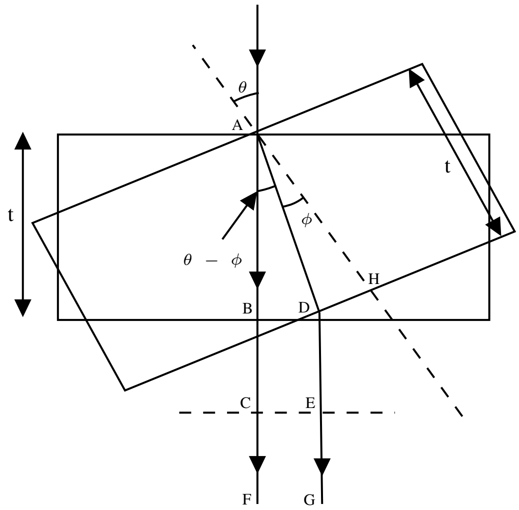

Figure 4: Diagram showing the optical path of a light beam at normal incidence and when the glass slide is rotated by an angle θ. Here, t is the thickness of the glass slide and ϕ is the angle of refraction.

If a glass side that has a refractive index n is placed along the path of one of the beams of light in a Michelson interferometer, there will be an change in the optical path. By rotating the slide by a small angle, the change in the optical path will lead to a fringe shift that, if appropriately counted alongside the angle by which the slide is rotated, would allow for the calculation of the refractive index of the glass slide [4]. The starting point is to determine the difference in the optical path of the light beam. This can be better visualised using Figure 4. At normal incidence, the optical path followed by the light beam is

$$nAB + BC, \tag{12}$$

where n is the refractive index of the glass. When the slab is tilted by an angle θ, the optical path is

$$nAD + DE. \tag{13}$$

From Equations (13) and (12), the change in the optical path, denoted by δ is determined to be

$$\delta = nAD + DE - nAB - BC \tag{14}$$

In order to proceed further, it can be noted that a result from optics states that for monochromatic light of wavelength λ,

$$2\delta = N\lambda, \tag{15}$$

where N is the number of fringes that are shifted when the glass slide is rotated. There is a factor of 2 because the light travels the glass slide twice. Combining Equations (15) and (14), the following result is obtained:

$$2(nAD + DE - nAB - BC) = N\lambda. \tag{16}$$

Straightforward geometry from Figure 4 allows for expressing AD, DE, AB and BC in terms of the angle θ, the angle of refraction ϕ and the thickness of the glass slide t. These are given below:

$$AD = t\sec(\theta), \tag{17}$$

$$DE = t\sec(\phi)\sin(\theta - \phi)\tan(\theta), \tag{18}$$

$$AB = t, \tag{19}$$

$$BC = t\sec(\theta) - t. \tag{20}$$

Using the equations above, Equation (16) can be rewritten into the following equation [6]:

$$n = \frac{(2t - N\lambda)(1 - \cos\theta)}{2t(1 - \cos\theta) - N\lambda}. \tag{21}$$

Equation (21) suggests a non-linear relationship between N and θ. Rewriting the above equation with N as the subject, the following expression is obtained:

$$N = \frac{2t}{\lambda}\left(1 + \frac{n\cos\theta}{1 - n - \cos\theta}\right). \tag{22}$$

From the above equation, it is immediate that the relationship between N and θ is indeed non-linear. This is further ascertained from the figure below that is a plot of N against θ, where n, t and λ were chosen with an appropriate order of magnitude.

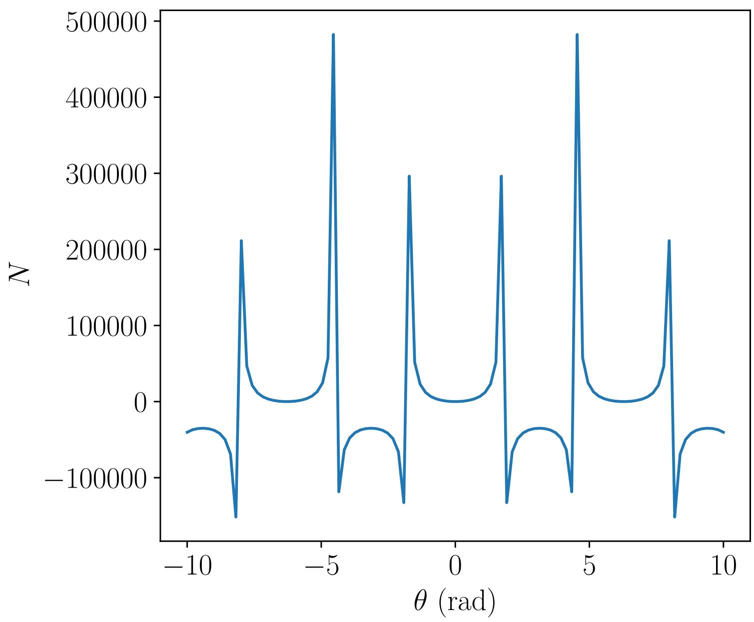

Figure 5: Plot of N against θ according to Equation (22)

4.2 Experimental Procedure

4.2.1 Overview

A glass slide whose index of refraction is to be determined is placed between M2 and BS as shown in Figure 1. The slide is mounted onto a rotational stage that allows for varying the angle θ in Equation (21). The thickness t of the slide is measured using a micrometer and recorded before placing it on the rotational stage. A reference point is fixed on the screen where the fringes are visible, and the number of fringes that pass through that point are counted as the rotational stage is rotated. 3 values of θ are fixed: $4°$, $8°$ and $12°$. For each θ, a value of N are determined. This procedure is repeated 5 times. The average N value is determined for each θ. Equation (21) can then be utilised to determine 3 values for n, which are averaged over to obtain the final measurement.

4.2.2 Error Analysis

The sources of uncertainty in n, from Equation (21), are straightforward to see. The uncertainty is λ has already been determined. There are also uncertainties in θ and t due to the least counts in the rotational stage as well as the micrometer respectively. Hence, each of the 3 values of n that will be determined from Equation (21) will have a propagated uncertainty given by the general formula in Equation (8). More specifically, each value of n will have an uncertainty given by the expression

$$u_n^2 = \left(\frac{\partial n}{\partial t}\right)^2 u_t^2 + \left(\frac{\partial n}{\partial \theta}\right)^2 u_\theta^2 + \left(\frac{\partial n}{\partial \lambda}\right)^2 u_\lambda^2. \tag{23}$$

Furthermore, since there is an averaging over values of n determined in 3 similar trials, there will be a standard uncertainty associated with the average value that will be determined. This standard uncertainty is given by

$$\alpha = \frac{\sigma_{N-1}}{\sqrt{N}}, \tag{24}$$

where

$$\sigma_{N-1} = \sqrt{\frac{1}{N-1}\sum_{i=1}^{N}(x_i - \bar{x})^2}, \tag{25}$$

where x_i is the i^{th} data point, $\bar{x}$ is the mean value of the data and N is the number of trials performed [2]. The total uncertainty in n will be given by

$$u_T^2 = \alpha^2 + u_n^2. \tag{26}$$

4.3 Experimental Results

The thickness t of the glass slide was measured to be

$$t = (0.001740 \pm 0.000003)\text{m}. \tag{27}$$

The following table summarises the results that were obtained for each trial and each value of θ. The value of n for each θ is also included in the table alongside the propagated uncertainties in each n value.

$\theta(^\circ)$	N_1	N_2	N_3	N_4	N_5	n
4.0 ± 0.2	1	2	2	1	1	1.36 ± 0.28
8.0 ± 0.2	13	9	9	10	10	1.92 ± 0.06
12.0 ± 0.2	22	15	19	21	20	1.68 ± 0.04

Table 2: Measurements of the angle θ at which the glass slide was rotated, fringe shift N and the resultant refractive index using Equations (27) and (21)

Using the above table of values, the average measurement of n and the standard uncertainty is

$$1.65 \pm 0.16. \tag{28}$$

Using Equation (26), the final measurement for the refractive index is

$$n = 1.65 \pm 0.33. \tag{29}$$

4.4 Discussion of Experimental Results

The experimental value of the refractive index was compared with the already known value of 1.5. This resulted in a 10% discrepancy between the observed value and the true value. Some of the uncertainties within the experimental procedure that could have led to this discrepancy include:

1. The speed at which the fringe shift was observed, which made it difficult to measure N accurately.
2. The stability of the optical breadboard.
3. The human reaction error in measuring N.
4. The small range within which θ was varied; a potential improvement would involve measuring over angles up until 360°.

5 Conclusion

The vast field of optical interferometry is introduced to students by means of simple experiments with the Michelson Interferometer. They allowed for a better understanding of various concepts in optics including determination of optical path differences, interference of light beams and the basics of coherence theory. These would only be strengthened if further experiments with the interferometer were conducted.

References

[1] Abdul Al-Azzawi. *Physical Optics: Principles and Practices*. CRC Press, 2006. ISBN: 978-0849382970.

[2] Ifan Hughes, Thomas Hase. *Measurements and Their Uncertainties: A Practical Guide to Modern Error Analysis*. Oxford University Press, 2010. ISBN: 978-0199566334.

[3] Eugene Hecht. *Optics*. Pearson Education, 2015. ISBN: 978-0133977226.

[4] George S. Monk. *Light: Principles and Experiments*. McGraw-Hill, 1937.

[5] Jeremy Ong. *Investigations of Light with a Michelson Interferometer*. Cornell University, 2010.

[6] *The Michelson Interferometer and the Hydrogen-Deuterium Isotope Shift*. Knox College Physics 341 - Advanced Physics Laboratory.

[7] Wikipedia. *Covariance Matrix*.